Atmos. Chem. Phys. Discuss., 9, 11501–11549, 2009
www.atmos-chem-phys-discuss.net/9/11501/2009/

Atmospheric Chemistry and Physics Discussions

This discussion paper is/has been under review for the journal *Atmospheric Chemistry and Physics (ACP)*. Please refer to the corresponding final paper in *ACP* if available.

Using ground-based solar and lunar infrared spectroscopy to study the diurnal trend of carbon monoxide in the Mexico City boundary layer

W. Stremme, I. Ortega, and M. Grutter

Centro de Ciencias de la Atmosfera, Universidad Nacional Autónoma de México, Mexico City, Mexico

Received: 24 February 2009 – Accepted: 24 April 2009 – Published: 8 May 2009

Correspondence to: W. Stremme (stremme@atmosfera.unam.mx)

Published by Copernicus Publications on behalf of the European Geosciences Union.

Abstract

Carbon monoxide (CO) is a main pollutant in urban agglomerations. Quantifying the total burden of this pollutant in a megacity is challaging because not only its surface concentration but also its vertical dispersion present different behaviours and high variability. The diurnal trend of columnar CO in the boundary layer of Mexico City has been measured during various days with ground-based infrared absorption spectroscopy. Daytime CO total columns are retrieved from solar spectra and for the first time, nocturnal CO total columns using moonlight have been retrieved within a megacity. The measurements were taken at the Universidad Nacional Autónoma de México (UNAM) campus located in Mexico City (19.33° N, 99.18° W, 2260 m a.s.l.) from October 2007 until February 2008 with a Fourier-transform infrared spectrometer at 0.5 cm^{-1} resolution. The atmospheric CO background column was measured from the high altitude site Altzomoni (19.12° N, 98.65° W, 4010 m a.s.l.) located 60 km southeast of Mexico City. The total CO column within the city presents large variations that are caused mainly by fresh CO emissions at the surface, but also the transport of cleaner or more polluted air masses within the field-of-view of the instrument and other processes contribute to its variability. The mean background value above the boundary mixing layer was found to be around $(1.2\pm0.2)\times10^{18}$ molecules/cm^2, while inside the city, the late morning mean on weekdays and Sundays was found to be $(3.2\pm0.3)\times10^{18}$ molecules/cm^2 and $(2.1\pm0.4)\times10^{18}$ molecules/cm^2, respectively. Continuous CO column retrieval during the day and night (when available), in conjunction with surface CO measurements, allow for a reconstruction of the effective mixing layer height. The limitations from this simplified approach, as well as the potential of using continuous column measurements in order to derive top-down CO emissions from a large urban area, are discussed. Also, further monitoring will provide more insight in daily and weekly emission patterns and a usable database for the quantitative validation of CO from satellite observations in a megacity.

ACPD

9, 11501–11549, 2009

1 Introduction

Ambient concentrations of carbon monoxide (CO) are variable and have changed significantly since industrialization. CO is emitted into the atmosphere mainly from the combustion of fossil fuels, with the main contribution in urban areas coming from the transportation sector. Key reasons for investigating CO in the atmosphere are its danger to humen health and its role in tropospheric chemistry, particularly controlling the hydroxyl (OH) budget (Finlayson-Pitts et al., 1992; Forster et al., 2007). For more than one decade, there has been wide interest in investigateing the contribution of anthropogenic and biomass burning sources of CO to its observed global distributions. Insight into the amount, distribution, trends and variability of the CO burden on the global scale are available from surface in situ measurements, column and profile retrievals from remote ground sites and more recently from space (Rinsland and Levine, 1985; Pougatchev and Rinsland, 1995; Barret et al., 2003; Edwards et al., 2004; Yurganov et al., 2004, 2005, 2008; Sussmann and Buchwitz, 2005; Dils et al., 2006; Turquety et al., 2008; Clerbaux et al., 2008; Senten et al., 2008) and references therein. A recent study (Halland et al., 2008) presented how the CO profiles retrieved from a satellite, can be used to trace and identify convective vertical transport from the boundary layer to the free troposphere.

Accurate measurements of CO in Mexico City, the world's second most populated city, are critical in order to study its impact on human health and the environment. The emission sources of CO in Mexico City include traffic and industry. Since 1986, surface volume mixing ratios of CO have been measured in Mexico City by a government run automated network for atmospheric monitoring (Red Automatica de Monitoreo Ambiental (RAMA), http://www.sma.df.gob.mx/simat). The continuous monitoring of CO surface mixing ratios have led to policy that has lowered the pollution levels in Mexico City during the last ten years (Molina and Molina, 2002; Stephens et al., 2008; Official Inventory for 2004).

ACPD
9, 11501–11549, 2009

The average CO surface mixing ratios (1990–2006) (Stephens et al., 2008) confirm the trend in the annual CO emission (Official Inventory for 2000; Official Inventory for 2004; Official Inventory for 2006), but these do not satisfactorily correlate and there are still important discrepancies in the estimation of CO emissions based on bottom-up approaches (Official Inventory for 2000; Schifter et al., 2005). This encourages further investigations to be carried out to determine CO emissions with different methodologies.

The weekly and daily patterns of the estimated CO emissions differ from the pattern in the measured CO surface concentrations. The weekday with the highest estimated CO emission reported for 2006 is Saturday (Official Inventory for 2006), however the CO surface concentration is still slightly lower on Saturdays as on normal working days (Stephens et al., 2008). The daily pattern in the CO surface concentration (main peak at 8:00 Local Time (LT, GMT-6 h) and local minimum at 15:00 LT) does not correlate with the diurnal CO emission and a direct proof of the diurnal CO emission in the inventory is not possible (Official Inventory for 2006; Stephens et al., 2008).

Even without horizontal CO transport, the emissions and vertical mixing of CO have direct impact on the concentrations near the surface. Large uncertainties in the mixing layer height can thus lead to significant deviations of model results. Additional knowledge of the total column thus provide valuable information of the total budget within the boundary mixing layer (de Foy et al., 2007). CO total columns have been derived before in Mexico City during 2003 from solar absorption measurements (de Foy et al., 2007). It was shown there that since vertical dispersion schemes in air quality models can have a large impact on simulated surface concentrations, the total column measurements of CO can be beneficial when used as constraint. During the MILAGRO/INTEXB campaign in 2006, solar absorption measurements with a higher resolution FTIR spectrometer where performed (J. Hannigan, personal communication, 2008). These measurements were taken northeast of Mexico City (T1 site in Tecamac) and during that study, the vertical structure of the boundary layer and its diurnal cycle was characterized using various instruments (Shaw et al., 2007). Solar FTIR re-

trievals are very sensitive to various instrumental properties and retrieval settings, so that side-by-side comparisons can be very useful in order to increase the confidence of the measurement technique. Unfortunately, the above mentioned experiments did not coincide with this study and their results can only be used as a reference to the current study. For this reason, special effort has been taken to assess the errors and presicion of the results presented here (Sect. 4.5).

This paper presents the retrieved total column of urban carbon monoxide measured during daytime from solar infrared spectra and for the first time, the CO column in a megacity has been measured during the night from a ground-based instrument. Both type of measurements, when the conditions are satisfied, provide a continuous time series of the column which provides new insight into the nocturnal structure of the atmosphere. Using this information, diurnal patterns of the CO budget are investigated during different periods, the height and evolution of the mixing layer can be monitored under specific conditions and a new approach for estimating the effective emission of CO in Mexico City is proposed. The gained knowledge from the CO column and its variability and trends opens the possibility for further improvements in photochemical models and the validation of the "hot spots" measured from satellites over the regions with major urban centers as MOPITT (Massie et al., 2006; Clerbaux et al., 2008), SCIAMACHY (Buchwitz et al., 2007), TES (Rinsland et al., 2006) and IASI (Barret et al., 2005).

A recent validation study using aircraft born measurements (Emmons et al., 2008) suggests that the new retrieval version 4 of MOPIIT data will be able to handle high polluted regions for the first-time with columns above 4.0×10^{18} molecules/cm^2 and thus new validation efforts will be needed.

2 Measurement realization

The CO column measurements were taken at the Universidad Nacional Autónoma de México (UNAM) campus (19.33° N, 99.18° W, 2260 m a.s.l.) in Mexico City between

ACPD
9, 11501–11549, 2009

October 2007 and February 2008. The UNAM site is in the south of the city, as shown in Fig. 1, and is surrounded by several surface CO monitors from the local monitoring network (SIMAT, 2008[1]). Additionally, background column measurements of CO were performed during 29 November to 2 December 2007 at the Altzomoni high altitude research site (19.12° N, 98.65° W, 4010 m a.s.l.) located 60 km southeast of Mexico City, Fig. 1.

2.1 Instrumentation

The spectra were collected with a FTIR spectrometer (Bruker, Opag 22) with a nominal resolution of 0.5 cm^{-1} at a max. optical path difference (OPD) of 1.8 cm. The FTIR is equipped with a KBr beamsplitter and a cryo-cooled mercury-cadmium-telluride (MCT) detector. The field of view (FOV) of the instrument is 30 mrad but a telescope was used resulting in a FOV of 7.5 mrad. The system is coupled to a video camera and automatic scanning mirror that actively track the light coming from the sun and moon. The scanning device, which has been described in more detail elsewhere (Harig, 2004; Harig et al., 2005), searches for the position of the most intense radiation in a specific wavelength range in the following manner. First, a two dimensional area is defined around the source and a low spectral resolution scan (at 20 cm^{-1}) is carried out with a user-defined step size. The two stepper motors controlling the position of the scanning mirror performs a fast scan, which will only take a few seconds, and the mirror then moves to the pixel position where the highest light intensity was detected. The spectrometer then collects infrared spectra at a higher resolution of 0.5 cm^{-1} at this position for a fixed amount of time and then performs a new fast scan centered at the last position chosen with the maximum intensity. This system was originally designed for passive detection of pollutants and the visualization of toxic substances (Harig et al., 2007) and has been also applied for characterizing the emissions of industrial plants

[1]Sistema de Monitoreo Atmosferico de la Ciudad de Mexico, available at: http://www.sma.df.gob.mx/simat/.

(Grutter et al., 2008a), airplanes (Flores-Jardines et al., 2005) and volcanoes (Grutter et al., 2008b).

2.2 Solar measurements

For solar absorption measurements, the scanner is optimized for tracking between 2700 and 3200 cm^{-1} and the system works well without frequent adjustments even when thin clouds are present. The solar angle changes at about 4.4 mrad/min so that with a FOV of 7.5 mrad, a new scan needs to be started after approximately one minute. About 60 usable spectra are recorded and averaged for further processing.

The MCT detector readily saturates when direct solar radiation is used. Therefore, the light is attenuated with a variable number of wire-mesh screens placed prior to the telescope. A disadvantage of using metal gratings at the entrance of the telescope (with 4 times magnification) is that the thermal emission of the mesh-filter interferes in the region between 800 and 2000 cm^{-1} and can influence the spectrum in the region of the CO evaluation. This thermal emission variates with the temperature of the grating and a three-step correction is applied to account for this interferance; First, a background spectrum is chosen from an in the laboratory created library of thermal emission spectra at different grating temperatures (the selection criteria are the correlation in the regions 620–700 and 1500–1650 cm^{-1}, where water vapor (H_2O) and carbon dioxide (CO_2) totaly absorb and removes the sunlight). In a second step, the background is scaled and corrected for offset before subtracting it from the measured radiance spectrum, Fig. 2. In the last step, the regions of total absorption in the atmosphere between 2000 and 2200 cm^{-1} are used to fit a straight line, which is then also subtracted from the measured spectra. This last correction removes additional effects from the thermal emission of the spectrometer and improves the spectral correction, especially in the region of evaluation, Fig. 2, inset.

The solar absorption measurements presented in this study were made between October 2007 and February 2008 from 08:30–17:30 LT. An attempt was made to record spectra on most working days with blue sky or thin cloud conditions. The intensity of

ACPD
9, 11501–11549, 2009

the recorded spectra, as well as sky images taken automatically after each tracking position, where used to further classify usable data.

2.3 Lunar measurements

The temperature distribution of the moon's surface is strongly variable, with around 400 K at the warmest points on the bright side and as low as 200 K on the dark side (Pugacheva and Shevchenko, 2000). The radiation of the moon consists of two parts, the reflection from the sun and the thermal emission of the moon itself (Notholt et al., 1993). Both parts have a different spectral distribution; The sun has its maximum near 20 000 cm^{-1} and the moon's thermal radiation has, according to its mean temperature, a maximum around 1000 cm^{-1}.

Below 2200 cm^{-1}, the thermal emission dominates the spectrum as shown in Fig. 3. Even though the reflected sun intensity recorded with our telescope and MCT detector shows a relatively low signal to noise ratio, Fig. 3 (around 2400 cm^{-1}), the thermal radiation integrated over the observed half sphere of the moon is sufficient for the CO evaluation during full moon and up to one week before and after. On the other hand, the measured atmospheric background radiation consists of thermal emission from the instrument, back-scattered thermal emission from the earth and self emission of the atmosphere. Depending on the lunar zenith angle and the time of the day, these will have different contributions that cannot be neglected, Fig. 3. The contribution of the background emission is realtively small during a full moon but it is still necessary to record background spectra in adequate time intervals. The background spectra were recorded approximately every hour towards a similar zenith angle of the moon.

Tracking of lunar radiation in this urban environment worked best in the spectral region between 2000 and 2200 cm^{-1}, because here the contrast between the moon and interferences from thin clouds is higher in this spectral region than in the spectral region near the maximum intensity of the moon (800 to 1000 cm^{-1}). However, a few days before and after full moon and during daylight, better tracking was obtained using a wider spectral region between 900 and 2200 cm^{-1}. Because of the relatively low

intensity available for tracking and measuring lunar absorption spectra, the tracking frecuency was increased to every 5 s resulting in an increased number of usable spectra for further averaging and processing. Tracking the moon in the infrared worked even during the moon eclipse on 21 February in 2008 and in the presence of daylight, which provided the possibility for comparing the results from simultaneous solar and lunar retrievals.

The procedure for preparing the moon spectra for the CO analysis is done in three steps: 1) The background spectra, which is valid for the particular time frame, is subtracted. 2) A second order polynomial is fitted to the region of total absorption around the CO band and is subsequently subtracted (the self-emission correction of the instrument is done according to Burton et al., 2001). 3) All spectra within a 10 minute time period, which have a sufficiently high signal-to-noise ratio are averaged.

3 CO column retrieval

The CO columns from solar and lunar absorption spectra in Mexico City were retrieved using the SFIT2 code (Pougatchev and Rinsland, 1995). This radiative transfer and profile retrieval algorithm is mainly used for the analysis of solar ground-based spectra from high-resolution instruments. As we will demonstrate, the use of this code for moderate-resolution spectra gives acceptable results for the goals of sought in this work.

The inversion of gas profiles with SFIT2 was originally based on "Optimal Estimation Theory" (OET) described by Rodgers (1976) and uses an a priori profile and a covariance matrix (**Sa**). The SFIT2 code (version rdrv.3.90) is able to read in a regularization matrix $\mathbf{R}=\mathbf{Sa}^{-1}$ so that the cognate constraint approaches suggested by Tikhonov (1963), Steck (2002), von Clarmann and Grabowski (2007) can be realized. The main difference in the mentioned retrieval-approaches are their goals, aiming either to get the best estimation for one single atmospheric state (OET) or to reduce systematic hidden a priori information for a later (time) series analysis (von Clarmann

ACPD
9, 11501–11549, 2009

and Grabowski, 2007). The constraint in ground-based solar retrievals or for NADIR sounders, for example, is crucial and different for each experiment (Eremenko et al., 2008; Emmons et al., 2008; Luo et al., 2007).

The atmosphere above the measurement site is described with 29 layers from 2.260 km up to 100 km using the temperature and pressure profiles from the continuous radiosoundings taken twice a day by the Servicio Meteorologico National in Mexico City (Servicio Meteorologico Nacional, 2008). The spectral resolution allows retrieval of only one independent quantity that describes the volume mixing ratios (VMR) of carbon monoxide in all layers. The constraint is designed following mainly the guidance by Steck (2002); von Clarmann and Grabowski (2007). The retrieval algorithm fits the measured spectra by shifting the VMRs of the lowest three layers (1.5 km) using the MOPITT-a priori (NCAR MOPITT, 2008), Fig. 5a. This constraint is motivated through the assumption that there are strong CO variations in the mixing layer. A Gauss-distribution as is normally assumed in the OET would lead to a systematic underestimation of pollution events, also recently mentioned by Emmons et al. (2008). A freely adapted VMR value in the boundary layer region reflects the typical situation in Mexico City and when compared to a simple profile-scaling constraint, results in a lower smoothing error (Sect. 4.1) and also improves the averaging kernel in the region of interest, Fig. 5.

The spectroscopic line data are taken from the HITRAN 2004 compilation (Rothman et al., 2005) and for the sun spectra, we use the integrated solar model from (Hase et al., 2006). The whole spectral region between 2110 to 2160 cm^{-1} is fitted. There are several reasons for using a wide spectral range in this particular case as opposed to several narrower windows as is more commonly done (Pougatchev and Rinsland, 1995; Barret et al., 2003; Yurganov et al., 2004; Sussmann and Buchwitz, 2005; Velazco et al., 2005; Fokeeva et al., 2007; Kramer, 2006; Senten et al., 2008). The reduced resolution of the spectra encourages a compromise between single line retrieval and band retrieval. The single or few line retrievals have the advantage, that the time for processing one spectrum is comparably small and a reasonably good fit can be realized.

ACPD
9, 11501–11549, 2009

This is desirable as the forward-model error indicated solely by a systematic residual cannot be quantified. However, in this study the resolution does not allow for an easy estimation of the back-line, because the individual lines sit on a socket (the smoothed CO-band). Spectra with 0.5 cm^{-1} resolution do not show completely separated CO absorption lines and there is also a significant interference of CO_2, H_2O and Ozone (O_3) in this region. A wide spectral region contains more information (Echle et al., 2000) and improves the estimation of the background slope and the columns of the interfering species. The spectral window of 50 cm^{-1} chosen for this study seems to contain sufficient information and is a good compromise to the computational requirements.

4 Retrieval diagnostics and error estimation

Although this study focuses on the variability and trends of the CO column observed above Mexico City, an analysis and quantification of the main error sources are necessary in order to identify the potential improvements to be done in the analysis, understand its limitations and determine the use of the retrieved columns, i.e. using the CO columns in photochemical models or for satellite validation purposes.

Error analysis in remote sensing retrievals is an current topic. Many different errors have to be discussed as they can play a role in the accuracy and in the precision of the retrieval (Rodgers, 1990, 2000; von Clarmann et al., 2001; Sussmann and Borsdorff, 2007). Here we will discuss briefly systematic errors: smoothing error, temperature error, errors resulting from the instrumental line shape (ILS), and spectroscopic errors. The resulting precision is estimated from the retrieved columns.

4.1 Smoothing error

To evaluate how in average the constraint retrieval differs from the true state, the smoothing error ϵ_{smooth} is calculated (Rodgers, 1990). (If more than one independent

qunatities are available, the error is better described by the matrix $\mathbf{S}_{\text{smooth}}$).

$$\mathbf{S}_{\text{smooth}} = (\mathbf{A} - \mathbf{1})\mathbf{S}_{\mathbf{a}}(\mathbf{A} - \mathbf{1})^{t} \quad (1)$$

$$\epsilon_{\text{smooth}} = \sqrt{\mathbf{S}_{\text{smooth}}} \quad (2)$$

The total column averaging kernel (**A**) is shown in Fig. 5b (red curve for the used retrieval). The covariance matrix ($\mathbf{S}_{\mathbf{a}}$), which describes the variability of the CO profiles, has to be estimated in order to calculate the smoothing error. Two different and statistically independent phenomena can lead to a variation of the CO profiles motivating two different estimations of the smoothing error: a) Through variations in the CO emissions, in the mixing layer height and in local dynamics which leads to a strong variability of CO in Mexico City. b) Through regional transport phenomena and changes of the CO profiles over wider areas due to for example biomass burning. The smoothing error in the column $\epsilon^{a}_{\text{smooth}}$ is calculated for case a) phenomena using a "2-parameter" ensemble of possible CO profiles constructed with the retrieved mixing layer height and the CO surface concentrations (the average of the 5 nearest in situ CO measurements). The effect of the variance in the regional background (case b) of CO on $\epsilon^{b}_{\text{smooth}}$ is estimated using an alternative covariance matrix (see Table 1), constructed from the MOPITT profiles (NCAR MOPITT, 2008). The profile for the ensemble consists of retrieved CO profiles (v.5.93) for the winter of 2007/2008 in the area between 17–21° N and 90–105° W. In Table 1 the resulting smoothing errors from the chosen constraint ("block VMR") and for a "profile-scaling" constraint are presented. The chosen CO retrieval reproduces the CO amount and its diurnal cycle in the mixing layer quite well (error is less than 5%) and the influence of the regional CO variance seems also to be minimized.

4.2 Temperature error

The temperature error, which may be classified as random for a time series based on daily mean, can be systematically influenced by solar heating affecting the retrieved diurnal cycle of the CO column. This error was estimated by retrieving the same

ACPD
9, 11501–11549, 2009

spectrum with different temperature profiles. The assumed temperature influences the retrieved CO columns in two ways: a) The absorbance of each molecule changes because the population of the lower state of an absorbing line depends on the temperature and b) the assumed air densities assumed in the layers vary with temperature. Both parts are separated input parameters in SFIT2 and they have their contrary effects on the retrieved columns. For a 5 K increase in temperature at a SZA=42, the CO column changes by +2.14% and by −1.96% due to changes in the absorption by molecules and the air density, respectively. The resulting effect on the retrieved CO column due to this change in temperature is ∼0.2%. Finally, both temperature effects cancel each other and the retrieved CO column is rather independent of the temperature profile for the used spectral window.

4.3 Error in the ILS

The instrumental line shape (ILS) plays an important role in FTIR spectroscopy, especially with a rather low resolution of 0.5 cm^{-1}. Previous studies on a similar spectrometer have shown that the ILS results from a rather triangular and slightly asymmetric apodization (Harig et al., 2005; E. Flores-Jardines, personal communication, 2007). Some studies to optimize the retrieval-strategy and evaluate the error related to the ILS have been done. As will be explained below, the ILS of the used interferometer can be described in a sufficiently accurate and stable manner with a triangular apodization function (with OPD 1.8 cm) in the observed spectral region.

The efforts were aimed to clarify a) how can the ILS be described in the SFIT2 retrieval, b) how large is the error resulting from an assumed (synthetic) ILS, c) is the ILS sufficiently constant and d) what parameter dominates the ILS. To ensure compatibility with the input of SFIT2, we used LINEFIT v.11 (Hase et al., 1999) to answer the above questions. CO absorptions lines were used for the ILS analysis. Previous studies used the CO absorption line to conduct the ILS analysis for similar instruments (Harig et al., 2005; Flores-Jardines, 2008; Horrocks et al., 2001). Different tests were carried out in the field (with high CO pressures) and in the laboratory (with low CO pressure). The

ACPD
9, 11501–11549, 2009

LINEFIT code was used to retrieve the ILS and an apodization function described by 40 numbers. The obtained apodization function has a slightly asymmetric triangular shape. The results using different spectral windows were slightly different.

The size of the ILS-error was studied in the following manner. Using the retrieved (assumed true) ILS, a forward simulation for a typical CO column (col_{true}) was done and then the CO column was retrieved col_{ret} with a triangular apodization function. The relative error ϵ_{ils}, Eq. (3),

$$\epsilon_{ils} = (col_{ret} - col_{true})/col_{true} \quad (3)$$

was evaluated for different ILS-retrievals obtained from different spectral windows and different experiments. The typical column difference for the two resulting ILS retrievals was found to be up to 4% for the ILS measured in the field (with relativly high CO pressure) and always below 2% for the laboratary measurements. The evaluation showed that using many CO lines, similar to what is done in the retrieval of the atmospheric columns, the obtained ILS can be replaced by the ILS of a triangular apodization without a strong effect on the retrieval results. That is to say, by using a directly retrieved ILS (40 numbers) in the column retrieval shows in the average no clear improvement in the residuals. Therefore the simplified ILS resulting from a symmetric triangular apodization was adopted.

Three reasons justify using the simplified ILS: i) The ILS retrieval from cell measurements contains systematic errors like for example such as a difference in the divergence of the non-perfect collimated light sources between lamp (or sun/moon with metal-mesh filter) and the spectrometer resulting in an uncertainty of the valid apodization function. ii) Misalignment of the used telescope can lead to small changes in the ILS and the accurately described ILS might not be valid for the entire time series. And iii) the reconstruction of the ILS is a mathematically ill-posed problem, and different constrains, parameterization and spectral regions result in similar but also slightly different ILS retrievals. Specially as in our case, the non-fitted parameter FOV seems to be the most unknown quantity.

4.4 Random errors

Random errors affect the precision of the measurement technique. They are by definition randomly different in each measurement and occur due to spectrum preparation, cloud conditions and the noise. Random errors can be reduced by the factor $1/\sqrt{N}$ (Poisson statistics) by averaging N spectra or their retrieval results. We call the spectra which are prepared for a retrieval to be a measurement. For solar measurements, each recorded spectrum is analyzed individually because the random noise is rather small due to the low resolution of the instrument (Harig, 2004). In the case of the lunar measurements, which have a smaller signal, the spectra are averaged over a ten minute interval to increase the signal-to-noise ratio.

The random error of a fixed time intervall can be used to compare the precision of this measurement technique with others. To estimate the random error for the solar measurements we evaluate the variability of the retrieved columns over a short time interval. A random error for a single measurement of 5% was estimated by the averaged difference of consecutive measurements and the random error for an hourly mean (≈33 spectra) was 1.0%. This number corresponds to the average of all time intervals. In the time interval of an hour, first a fited straight line is subtracted and the standard error is then calculated.

4.5 Experimental evaluation of the retrieved CO column

The precision is estimated from a series of measurements as in the previous section. This does not give insight into sources of errors, but it gives a reliable information about the quality of the measurement.

The calculated total systematic errors in the CO column consists of different particular addressed errors. All these errors are based on estimated variabilities and uncertainties. The results shown in Table 2 show that the ILS seems to be the most important error source and limits the accuracy of the measurement. However, the error analyzis in this bottom-up manner is not always complete or correct.

To check if the CO column retrieval from solar spectra is overall a good result and to ensure that no important error sources are missing, an additional experiment was done. The cylindrical housing of the telescope was closed by a film that is transparent in the infrared and for a time period when the SZA did not change significantly, a large amount of CO was injected into the semi-closed cell. The injection with approximately equal amounts of CO was repeated every minute during the sun-tracking phases. Figure 6a shows, as expected, a linear increase in the retrieved CO column and the correlation shows that the retrieval is performing well. The slope of the correlation plot in Fig. 6b should be equivalent to the lowest layer averaging-kernel element. Normally, the averaging kernel $\mathbf{A}=\partial \mathrm{col}_{\mathrm{ret}}^{\mathrm{CO}} / \partial \boldsymbol{x}_{\mathrm{true}}^{\mathrm{CO}}$ is calculated using the same forward model as in the retrieval. In the designed experiment, however, the forward simulation is done experimentally and therefore the forward model and the ILS can be evaluated. This experiment is limited by the estimation in the amount of injected CO and the free volume in the telescope housing. The linear behavior between the retrieved and the injected column over a wide range, however, shows a good agreement between the estimated and retrieved CO column confirming the reliability of the results.

A study with the ILS showed that if there is a systematic difference between assumed and true ILS; the relation between retrieved and true column is not certainly linear for a wide range. This control experiment proves the linear response of the CO retrieval, shows no significant biases and thus validates the retrieval set-up.

5 Results

The CO column was measured in Mexico City between October 2007 and February 2008 and the results are presented in this section. The total column can change according to three main, independent mechanisms: 1) A regional variability that can also be detected outside the urban area due to changes in global composition, annual variability or the influence from other sources such as biomass burning. 2) The anthropogenic emission of CO within the metropolitan area, which should present a diurnal

ACPD
9, 11501–11549, 2009

pattern but might vary from day to day. 3) The local and regional meteorological conditions responsible for air flow patterns that affect the pollutant concentrations above the measurement site.

In the first part (Sect. 5.1), measurements that have been taken above the boundary layer are presented. These measurements were performed in order to gain more knowledge about which part of the measured total column belongs to the regional background levels and which can be attributed to the urban air within the mixing layer of Mexico City. In Sect. 5.2, the daily means of 50 days during the measurement period are shown in order to identify patterns and possible differences between working days and weekends. Additional coincident information of the measured surface concentration of CO is used in Sect. 5.3 to study the diurnal patterns of column and ground-level CO and to reconstruct an effective mixing layer height, which is then compared with model results.

5.1 Total CO column measurements above the boundary layer

Solar and lunar absorption spectra have been recorded at the high-altitude remote site of Altzomoni, located 60 km south east of Mexico City and at 4010 m a.s.l. From these spectra, the total CO column is obtained with a similar retrieval strategy as for spectra taken in Mexico City. Only the constraint was adapted to the assumption that Altzomoni is above the mixing layer and an enhancement in the free troposphere is well represented by a scaling of the a priori profile. A test shows that if in contrary to the presented profile-scaling-retrieval only the lowest two layers (1 km) are allowed to freely adapt, the resulting columns are systematically 5% lower.

The results of the measurements done between 29 November and 2 December 2007 are presented in Fig. 7. There were blue sky conditions during the mornings with some clouds in the afternoons. At night the sky was typically clear, although the moon measurements were sensitive to thin clouds and the available radiation was limited (on 30 November only about 60% of the surface was illuminated). It can be observed that the CO column increases in the midday and early afternoon. This suggests that

the mixing layer rises above 2 km and that the urban pollution reaches the Altzomoni site. This is in agreement with a recent study that presents the properties of gases and aerosols at this same research site (Baumgardner et al., 2009). In this study, the anthropogenic influence detected particularly during the afternoons originates from all surrounding regions and not only when the wind comes from the Mexico City area.

From the results presented in Fig. 7 and previous studies at this research site, one can assume that the Altzomoni site is usually above the convective mixing layer before noon. In Table 3, the results from the average total columns obtained both from lunar and solar measurements (between 09:00–12:00 LT), are presented. The mean value of $(1.2\pm0.08)\times10^{18}$ molecules/cm^2 is in the expected range for this latitude and altitude which is based on other high altitude CO measurements from NDACC stations in the Northern Hemisphere as for example (Izana 28° N, 2360 m a.s.l., Jungfraujoch 47° N, 3580 m a.s.l., Zugspitze 47° N, 2964 m a.s.l.) for this time of the year (Gardiner et al., 2007; Kramer, 2006). A background lower limit of the CO column (col^{co}_{altz})$=1\times10^{18}$ molecules/cm^2, corresponding to clear air in the region above 4 km altitude is used as reference for future analysis and is expected to have a variablitity smaller than 20%.

The early morning (08:00 LT) of 1 and 2 December shows an enhancement of the CO column that disappears around 09:00 LT. This has also been observed on some days from column measurements recorded in Mexico City, Fig. 11. It is unlikely that this enhancement is due to an artifact coming from a high SZA since not all days present this feature. Therefore, a more likely explanation is the presence of a residual layer that slowly diappeares in the morning.

5.2 Daily variations of the CO columns within Mexico City

The daily CO columns measured at the UNAM site in Mexico City from October 2007 to Febrary 2008 are presented in Fig. 8. The data, expressed as daily mean values recorded during the 09:00–12:00 LT time periods, comprise 45 working days including Saturdays. The mean column measured during the period was

ACPD
9, 11501–11549, 2009

$(3.2\pm0.3)\times10^{18}$ molecules/cm^2. The standard deviation (STDEV) within a working day was on average about 25%. We include Saturdays in the working days, as in recent time the traffic conditions and the estimated CO emissions on Saturday are similar to normal working days (Official Inventory for 2006). If the data collected on Saturdays are excluded from the data set, the average CO total column differs by only 0.3%.

It is evident from the data that, on days with efficient ventilation (emissions are assumed to persist), the total column approximates the background value of 1.2×10^{18} molecules/cm^2. The total CO column amount above Mexico City is thus strongly dependent on the wind condition, as can be seen from the large day-to-day variability in Fig. 8. This has also been observed in a time series recorded in Moscow (Fokeeva et al., 2008).

Data was also collected on 5 Sundays during the measurement period. The average total column was found to be $(2.1\pm0.4)\times10^{18}$ molecules/cm^2, which is 35% lower than the average of the working days. In Fig. 9 the data is presented according to the day of the week. Here the effect that reduced emissions have on the total columns is clearly seen.

The values measured are consistent with CO total column values reported previously in the region. During 2003, total columns of $(2–5)\times10^{18}$ molecules/cm^2 were measured near downtown Mexico City (de Foy et al., 2007) and during the MILAGRO field campaign in 2006, a mean value of (1.74×10^{18} molecules/cm^2) was measured at the T1 research site (Tecamac), located 50 km north east outside of Mexico City (J. Hannigan, personal communication, 2008). The CO column daily means recorded in Mexico City are similar to the typical CO column above Moscow (156 m a.s.l.). Here a mean column of $\approx3.5\times10^{18}$ molecules/cm^2 (Fokeeva et al., 2007) resembles the values of Mexico City except that both cities have far different surface pressures.

ACPD
9, 11501–11549, 2009

5.3 Diurnal patterns and MLH estimation

Especially for Mexico City the convective mixing layer height (MLH) and its dynamics plays a key role in air quality. The in situ measurements of the CO surface concentrations show a completely different diurnal behavior than the CO column, as shown in the example presented in Fig. 10. Even though surface concentrations and column measurements are dependent on wind conditions and changes in emissions, both are different quantities and a direct comparison is not possible without knowledge of the vertical structure of the atmosphere. In the mornings, a convective mixing layer is formed and CO accumulates near the surface when the highest in situ concentration is measured. The MLH, driven by solar heating (Whiteman et al., 2000), grows and the CO concentration decreases at the surface, regardless if the total CO column stays constant or increases on a typical day.

If the convective mixing layer is well defined, the vertical CO-profile consists of two parts. The "normal" clean air CO profile above the mixing layer and a part with a nearly constant volume mixing ratio of CO (VMR_{co}) between surface and upper boundary of the mixing layer Z_{MLH}. The assumption of a homogeneous mixing within the layer is the simplest approximation, but is also motivated by the short mixing time and the relatively long lifetime of CO. Even if the mixing layer is not homogeneous, the retrieved effective Z_{MLH} is a usefull quantity to derive from the atmospheric CO column. (Similarly, the tropospheric and stratospheric columns of nitrous oxide (N_2O), methane (CH_4) and hydrogen fluoride (HF) have been separated by retrieving an effective tropopause height from ground-based solar absorption spectra (Stremme, 2007) and the tropospheric nitrogen dioxide (NO_2) column can be derived (Sussmann et al., 2005) from a combination of space borne and ground-based column retrievals.)

The total CO column (col_{co}^{mex}) can be written as the sum of two parts Eq. (4),

$$col_{co}^{mex} = \int_0^{Z_{MLH}} VMR_{co} \cdot \rho_{air}(z) dz + col_{co}^{altz}, \quad (4)$$

Where Z_{MLH} is the location of the MLH above surface, VMR_{co} is the volume mixing ratio

ACPD
9, 11501–11549, 2009

of CO, $\rho_{air}(z)$ represents the air density for the altitude z and col_{co}^{altz} is the background column of CO. The part above the MLH is estimated from the lower limit value measured at Altzomoni, $col_{co}^{altz} \approx 10^{18}$ molecules/cm^2, and the air density profile is provided by the daily radiosonde measurements. For determining a representative surface concentration around the UNAM site, the average of the surface CO VMR (hourly mean) of the 5 nearest monitoring stations (PLA, PED, TAX, SUR, UIZ) was calculated, Fig. 1, and to obtain a coincident VMR_{co} value, the CO surface volumn mixing ratios are linearly interpolated to the times of column measurements. The inversion of Eq. (4) to get Z_{MLH} is done by an IDL program for each column measurement.

Because CO is used in this case as a tracer for the MLH (similar to Halland et al., 2008), the reconstruction works better during time of high contamination. The resulting time series for Z_{MLH} are shown in Figs. 10–13. The retrieved MLH is independent of the CO concentration and the CO surface emissions (even if it is based only on CO measurements) and is therefore independent of the actual traffic conditions and should not show a weekly pattern. The reconstructed MLH and its typical diurnal cycle in Fig. 13 is consistent with results of other instruments characterizing the vertical structure of the boundary layer (Shaw et al., 2007) and model based studies (Fast and Zhong, 1998; Whiteman et al., 2000).

The same connection between MLH, column measurements and surface concentration in the Mexico City region has also been observed for example using NO_2 columns (Melamed et al., 2009). But especially in the afternoon and during the night time, the assumption of a well defined single mixing layer might not be valid and further investigation is necessary, Fig. 10. In such cases, the retrieved MLH has to be discussed more carefully since the following scenarios might be possible:

i) The coexistence of two or more different layers in the boundary layer – also reported from measurements on other locations (Wiegner et al., 2006; Emeis et al., 2008) – is not included in the the simplified model.

ii) A higher CO VMR in the surface-nearest layer than in a less contaminated, aged residual layer could explain a decrease in the estimated Z_{MLH} in the afternoon. The

formation of a new mixing layer explains the second peak in the surface concentration of CO (Stephens et al., 2008).

iii) The air near the surface might be clean at times, but a polluted CO residual layer may be present above. An inhomogeneity like that would result in an over-estimated height Z_{MLH} and could be a typical case in night time, for example on 25 February, Fig. 10.

When applying the MLH retrieval during different seasons of the year, the annual variability of the CO background in the free troposphere has to be taken into account. This was probably not necessary for the interval of the current study. The annual cycle of the CO column has not yet been studied for Mexico City and surroundings, but it might be somewhat less than the amplitude of 3E17 molecules/cm^2 measured at the Izana station (28° N) (Kramer, 2006). The relative annual cyle with maxima during the spring and minima during the autumn for this region, can be estimated from the MOPIIT v.3 data (NCAR MOPITT, 2008).

Figure 13 shows a comparison of the MLH (FTIR-retrieved) and the results from an operative model during the measurement period. The available model data are 3 h snappshots of the defined MLH calculated with a horizontal resolution of 32 km (NCEP, 2008[2]). All data are interpolated linearly to the time of the measurements. A similar mean and range of the variation in the MLH is found and for some days, a good correlation was obtained, Fig. 13b. For lower MLHs, the higher values of the model than the reconstructed MLH show a bias of about 700 m and slope of 0.5 with an overall correlation of R^2=0.37, Fig. 13. This result may be improved considerably if data with higher time resolution from the model would be available and the days with strong convective or ventilation processes are filtered out.

[2]Data available at: http://wwwt.emc.ncep.noaa.gov/mmb/rreanl/index.html.

ACPD
9, 11501–11549, 2009

6 Conclusions

In this work, the column densities of carbon monoxide in Mexico City are reported and their dirunal and daily patterns are presented. The total CO columns have been retrieved from solar and lunar infrared spectra measured with a low-cost instrumental set-up, which consists of a moderate-resolution FTIR spectrometer and a simple scanning device. The quantitative analysis used is described here and the most important error sources are evaluated. The results demonstrate that this experimental set-up can provide reliable information on the absolute column of CO and most relevant for this study, it can succesfully follow its evolution during the day. Also, the CO columns are measured for the first time in a megacity during the night using lunar absorption spectroscopy.

Using the initial data set of 50 days considered in this study during the winter 2007/2008, a significant difference is seen in the CO column between Sundays ($2.1\pm0.4\times10^{18}$ molecules/cm^2) and working days ($3.2\pm0.3\times10^{18}$ molecules/cm^2). The clearly observed weekly and diurnal patterns proves that it is possible to gain new informartion about the anthropogenic emissions from the column measurements. A typical background CO column of $(1.2\pm0.08)\times10^{18}$ molecules/cm^2 was estimated for this period from measurements carried out at the remote, high-altitude research site of Altzomoni (4010 m a.s.l. 60 km southeast of Mexico City). This background value was used to estimate which part of the columns measured in Mexico City is not part of the pollution within the mixing layer.

The high measurement frequency allowed for the investigation of diurnal and nocturnal behavior. The diurnal change of the CO column and its surface concentration do not correlate but they can complement each other and provide extra information about the vertical dispersion of CO. The mixing layer height (MLH) was reconstructed from the CO column and surface concentration measurements. The diurnal cycle of the reconstructed MLH shows the typical boundary layer behaviour (growth between 09:00–12:00 LT), which is a behavior well known based on model studies and mea-

ACPD
9, 11501–11549, 2009

surements from other instruments. The reconstruction, which is not valid for all times of the day, seems to work well when a single convective layer is present.

The ability to reproduce under special conditions the MLH evolution from only CO measurements, which is in essence independent of the pollution levels and the emission patterns in the city, opens the possibility for a top-down estimation of the CO emissions to be performed based on ground-based remote sensing measurements. Attempts to pursue this objective will be sought with a larger measurement period and additional observations so that the vertical structure and dynamics of the atmosphere can be better characterized. Also, this work shows the feasability for using total CO measurements at this sub-tropical location for the validation of satellite NADIR sounders. This simple experimental approach could be deployed in emerging megacities in other developing countries so that comparisons between the different populated cities, emissions from top-down estimations and for wider satellite validations can be realized.

Acknowledgements. We wish to thank Roland Harig for his support to realize the solar absorption measurements with the scanning infrared system (SIGIS) and important discussions. Victor Ramos from the Servicio Meteorologico National is acknowledged for providing the radiosonde data and Ernesto Caetano for the useful discussions and for preparing the model outputs for the MLH. We would like to thank also Jim Hannigan for his support with SFIT2 and for his help in the evaluations, as well for sharing his results from the MILAGRO/INTEXB campaign, and Frank Hase is thanked for his support with LINEFITv.11. We thank Megan Melamed for discussion and carfully reviewing.

References

Barret, B., De Mazière, M., and Mahieu, E.: Ground-based FTIR measurements of CO from the Jungfraujoch: characterisation and comparison with in situ surface and MOPITT data, Atmos. Chem. Phys., 3, 2217–2223, 2003, http://www.atmos-chem-phys.net/3/2217/2003/. 11503, 11510

Barret, B., Turquety, S., Hurtmans, D., Clerbaux, C., Hadji-Lazaro, J., Bey, I., Auvray, M., and Coheur, P.-F.: Global carbon monoxide vertical distributions from spaceborne high-resolution FTIR nadir measurements, Atmos. Chem. Phys., 5, 2901–2914, 2005, http://www.atmos-chem-phys.net/5/2901/2005/. 11505

Baumgardner, D., Grutter, M., Allan, J., Ochoa, C., Rappenglueck, B., Russell, L. M., and Arnott, P.: Evolution of anthropogenic pollution at the top of the regional mixed layer in the central Mexico plateau, Atmos. Chem. Phys. Discuss., 9, 3265–3306, 2009, http://www.atmos-chem-phys-discuss.net/9/3265/2009/. 11518

Buchwitz, M., Khlystova, I., Bovensmann, H., and Burrows, J. P.: Three years of global carbon monoxide from SCIAMACHY: comparison with MOPITT and first results related to the detection of enhanced CO over cities, Atmos. Chem. Phys., 7, 2399–2411, 2007, http://www.atmos-chem-phys.net/7/2399/2007/. 11505

Burton, M. R., Oppenheimer, C., Horrocks, L. A., and Francis, P. W.: Diurnal changes in volcanic plume chemistry observed by lunar and solar occultation spectroscopy, Geophys. Res. Lett., 28, 843–846, doi:10.1029/2000GL008499, 2001. 11509

Clerbaux, C., Edwards, D. P., Deeter, M., Emmons, L., Lamarque, J.-F., Tie, X. X., Massie, S. T., and Gille, J.: Carbon monoxide pollution from cities and urban areas observed by the Terra/MOPITT mission, Geophys. Res. Lett., 35, L03817, doi:10.1029/2007GL032300, 2008. 11505

Clerbaux, C., George, M., Turquety, S., Walker, K. A., Barret, B., Bernath, P., Boone, C., Borsdorff, T., Cammas, J. P., Catoire, V., Coffey, M., Coheur, P.-F., Deeter, M., De Mazière, M., Drummond, J., Duchatelet, P., Dupuy, E., de Zafra, R., Eddounia, F., Edwards, D. P., Emmons, L., Funke, B., Gille, J., Griffith, D. W. T., Hannigan, J., Hase, F., Höpfner, M., Jones, N., Kagawa, A., Kasai, Y., Kramer, I., Le Flochmoën, E., Livesey, N. J., López-Puertas, M., Luo, M., Mahieu, E., Murtagh, D., Nédélec, P., Pazmino, A., Pumphrey, H., Ricaud, P., Rinsland, C. P., Robert, C., Schneider, M., Senten, C., Stiller, G., Strandberg, A., Strong, K., Sussmann, R., Thouret, V., Urban, J., and Wiacek, A.: CO measurements from the ACE-FTS satellite instrument: data analysis and validation using ground-based, airborne and spaceborne observations, Atmos. Chem. Phys., 8, 2569–2594, 2008, http://www.atmos-chem-phys.net/8/2569/2008/. 11503

de Foy, B., Lei, W., Zavala, M., Volkamer, R., Samuelsson, J., Mellqvist, J., Galle, B., Martínez, A.-P., Grutter, M., Retama, A., and Molina, L. T.: Modelling constraints on the emission inventory and on vertical dispersion for CO and SO_2 in the Mexico City Metropolitan Area

ACPD

9, 11501–11549, 2009

using Solar FTIR and zenith sky UV spectroscopy, Atmos. Chem. Phys., 7, 781–801, 2007, http://www.atmos-chem-phys.net/7/781/2007/. 11504, 11519

Dils, B., De Mazière, M., Müller, J. F., Blumenstock, T., Buchwitz, M., de Beek, R., Demoulin, P., Duchatelet, P., Fast, H., Frankenberg, C., Gloudemans, A., Griffith, D., Jones, N., Kerzenmacher, T., Kramer, I., Mahieu, E., Mellqvist, J., Mittermeier, R. L., Notholt, J., Rinsland, C. P., Schrijver, H., Smale, D., Strandberg, A., Straume, A. G., Stremme, W., Strong, K., Sussmann, R., Taylor, J., van den Broek, M., Velazco, V., Wagner, T., Warneke, T., Wiacek, A., and Wood, S.: Comparisons between SCIAMACHY and ground-based FTIR data for total columns of CO, CH_4, CO_2 and N_2O, Atmos. Chem. Phys., 6, 1953–1976, 2006, http://www.atmos-chem-phys.net/6/1953/2006/. 11503

Echle, G., von Clarmann, T., Dudhia, A., Flaud, J.-M., Funke, B., Glatthor, N., Kerridge, B., López-Puertas, M., Martín-Torres, F. J., and Stiller, G. P.: Optimized Spectral Microwindows for Data Analysis of the Michelson Interferometer for Passive Atmospheric Sounding on the Environmental Satellite, Appl. Optics, 39, 5531–5540, 2000. 11511

Edwards, D. P., Emmons, L. K., Hauglustaine, D. A., Chu, D. A., Gille, J. C., Kaufman, Y. J., Pétron, G., Yurganov, L. N., Giglio, L., Deeter, M. N., Yudin, V., Ziskin, D. C., Warner, J., Lamarque, J.-F., Francis, G. L., Ho, S. P., Mao, D., Chen, J., Grechko, E. I., and Drummond, J. R.: Observations of carbon monoxide and aerosols from the Terra satellite: Northern Hemisphere variability, J. Geophys. Res., 109, D24202, doi:10.1029/2004JD004727, 2004. 11503

Emeis, S., Schäfer, K., and Münkel, C.: Long-term observations of the urban mixing-layer height with ceilometers, IOP Conference Series: Earth and Environmental Science, 1, 012027, doi: 10.1088/1755-1315/1/1/012027, 2008. 11521

Emmons, L. K., Edwards, D. P., Deeter, M. N., Gille, J. C., Campos, T., Nédélec, P., Novelli, P., and Sachse, G.: Measurements of Pollution In The Troposphere (MOPITT) validation through 2006, Atmos. Chem. Phys. Discuss., 8, 18091–18109, 2008, http://www.atmos-chem-phys-discuss.net/8/18091/2008/. 11505, 11510

Eremenko, M., Dufour, G., Foret, G., Keim, C., Orphal, J., Beekmann, M., Bergametti, G., and Flaud, J.-M.: Tropospheric ozone distributions over Europe during the heat wave in July 2007 observed from infrared nadir spectra recorded by IASI, Geophys. Res. Lett., 35, L18805, doi: 10.1029/2008GL034803, 2008. 11510

Fast, J. D. and Zhong, S.: Meteorological factors associated with inhomogeneous ozone concentrations within the Mexico City basin, J. Geophys. Res., 103, 18 927–18 946, doi:

10.1029/98JD01725, 1998. 11521
Finlayson-Pitts, B. J., Ezell, M. J., Jayaweera, T. M., Berko, H. N., and Lai, C. C.: Kinetics of the reactions of OH with methyl chloroform and methane – Implications for global tropospheric OH and the methane budget, Geophys. Res. Lett., 19, 1371–1374, doi:10.1029/92GL01279, 1992. 11503
Flores-Jardines, E.: Characterizacion de las emisones de turbinas de avion usando espectroscopia FTIR pasiva con un sistema de visualizacion, Ph.D. thesis, Universidad Nacional Autonoma de Mexico, 2008. 11513
Flores-Jardines, E., Schäfer, K., Harig, R., Rusch, P., and Grutter, M.: Investigation of temperature and gas concentration distributions in hot exhausts (airplanes and burners) by scanning imaging FTIR spectrometry, Proceedings of the SPIE, 5979, 365–376, 2005. 11507
Fokeeva, E. V., Grechko, E. I., Dzhola, A. V., and Rakitin, V. S.: Determination of carbon monoxide pollution of the atmosphere over Moscow with a spectroscopic method, Izv. Atmos. Ocean. Phy.+, 43, 612–617, 2007. 11510, 11519
Fokeeva, E. V., Rakitin, V. S., and Kuznetsov, R. D.: Carbon Monoxide Pollution Study of the Atmosphere over Moscow by à Spectroscopic Method, Geophys. Res. Abstr., 10, EGU2008-A-10311, 2008. 11519
Forster, P., Ramaswamy, V., Artaxo, P., Berntsen, T., Betts, R., Fahey, D., Haywood, J., Lean, J., Lowe, D., Myhre, G., Nganga, J., Prinn, R., Raga, G., Schulz, M., and Van Dorland, R.: Changes in Atmospheric Constituents and in Radiative Forcing, in: Climate Change 2007: The Physical Science Basis. Contribution of Working Group I to the Fourth Assessment Report of the Intergovernmental Panel on Climate Change, available at: http://www.ipcc.ch/pdf/assessment-report/ar4/wg1/ar4-wg1-chapter2.pdf (last access: 29 April 2009), 2007. 11503
Gardiner, T., Forbes, A., de Mazière, M., Vigouroux, C., Mahieu, E., Demoulin, P., Velazco, V., Notholt, J., Blumenstock, T., Hase, F., Kramer, I., Sussmann, R., Stremme, W., Mellqvist, J., Strandberg, A., Ellingsen, K., and Gauss, M.: Trend analysis of greenhouse gases over Europe measured by a network of ground-based remote FTIR instruments, Atmos. Chem. Phys., 8, 6719–6727, 2008, http://www.atmos-chem-phys.net/8/6719/2008/. 11518
Grutter, M., Basaldud, R., Flores, E., and Harig, R.: Optical Remote Sensing for Characterizing the Spatial Distribution of Stack Emissions, Advanced Environmental Monitoring, 107–118, 2008a. 11507

Grutter, M., Basaldud, R., Rivera, C., Harig, R., Junkerman, W., Caetano, E., and Delgado-Granados, H.: SO_2 emissions from Popocatépetl volcano: emission rates and plume imaging using optical remote sensing techniques, Atmos. Chem. Phys., 8, 6655–6663, 2008b. 11507

Halland, J. J., Fuelberg, H. E., Pickering, K. E., and Luo, M.: Identifying convective transport of carbon monoxide by comparing remotely sensed observations from TES with cloud modeling simulations, Atmos. Chem. Phys. Discuss., 8, 19201–19247, 2008, http://www.atmos-chem-phys-discuss.net/8/19201/2008/. 11503, 11521

Harig, R.: Passive Remote Sensing of Pollutant Clouds by Fourier-Transform Infrared Spectrometry: Signal-to-Noise Ratio as a Function of Spectral Resolution, Appl. Optics, 43, 4603–4610, 2004. 11506, 11515

Harig, R., Rusch, P., Schäfer, K., and Flores-Jardines, E.: Method for on-site determination of the instrument line shape of mobile remote sensing Fourier transform spectrometers, Proceedings of the SPIE, 5979, 432–441, doi:10.1117/12.627689, 2005. 11506, 11513

Harig, R., Matz, G., Rusch, P., Gerhard, H.-H., Gerhard, J.-H., and Schlabs, V.: Infrared remote sensing of hazardous vapours: surveillance of public areas during the FIFA Football World Cup 2006, Proceedings of the SPIE, 6538, 65381Z pp., doi:10.1117/12.720227, 2007. 11506

Hase, F., Blumenstock, T., and Paton-Walsh, C.: Analysis of the Instrumental Line Shape of High-Resolution Fourier Transform IR Spectrometers with Gas Cell Measurements and New Retrieval Software, Appl. Optics, 38, 3417–3422, 1999. 11513

Hase, F., Demoulin, P., Sauval, A. J., Toon, G. C., Bernath, P. F., Goldman, A., Hannigan, J. W., and Rinsland, C. P.: An empirical line-by-line model for the infrared solar transmittance spectrum from 700 to 5000 cm^{-1}, J. Quant. Spectrosc. Ra., 102, 450–463, 2006. 11510

Horrocks, L. A., Oppenheimer, C., Burton, M. R., Duffell, H. J., Davies, N. M., Martin, N. A., and Bell, W.: Open-path Fourier transform infrared spectroscopy of SO_2: An empirical error budget analysis, with implications for volcano monitoring, J. Geophys. Res., 106, 27 647–27 660, 2001. 11513

Kramer, I.: Zeitreihen troposphärischer Spurengase abgeleitet aus bodengebundenen FTIR-Messungen, Ph.D. thesis, Universität Karlsruhe, available at: http://digbib.ubka.uni-karlsruhe.de/volltexte/1000006009 (last access: 29 April 2009), 2006. 11510, 11518, 11522

Luo, M., Rinsland, C., Fisher, B., Sachse, G., Diskin, G., Logan, J., Worden, H., Kulawik, S., Osterman, G., Eldering, A., Herman, R., and Shephard, M.: TES carbon monoxide validation with DACOM aircraft measurements during INTEX-B 2006, J. Geophys. Res., 112, D24S48,

doi:10.1029/2007JD008803, 2007. 11510
Massie, S. T., Gille, J., Edwards, D. P., and Nandi, S.: Satellite observations of aerosol and CO over Mexico City, Atmos. Environ., 40, 6019–6031, 2006. 11505
Melamed, M. L., Basaldud, R., Steinbrecher, R., Emeis, S., Ruíz-Suárez, L. G., and Grutter, M.: Detection of pollution transport events southeast of Mexico City using ground-based visible spectroscopy measurements of nitrogen dioxide, Atmos. Chem. Phys. Discuss., 9, 4769–4804, 2009, http://www.atmos-chem-phys-discuss.net/9/4769/2009/. 11521
Molina, L. T. and Molina, M. J.: Air Quality in the Mexico Megacity: An Integrated Assessment, Kluwer Academic Publishers, Dordrecht, The Netherlands, 2002. 11503
NCAR MOPITT: CO profiles downloaded, available at: http://web.eos.ucar.edu/mopitt/, 2008. 11510, 11512, 11522
Notholt, J., Neuber, R., Schrems, O., and Clarmann, T. v.: Stratospheric trace gas concentrations in the Arctic polar night derived by FTIR-spectroscopy with the moon as IR light source, Geophys. Res. Lett., 20, 2059–2062, 1993. 11508
Official Inventory for 2000: Inventario de Emisiones a la Atmosfera, Zona Metropolitana del Valle de Mexico 2000, Gobierno del Distrito Federal, Secretaria del Medio Ambiente, available at: http://www.sma.df.gob.mx/inventario_emisiones/index.php?op=pub#(last access: 29 April 2009), 2003. 11504
Official Inventory for 2004: Official inventory: Inventario Emissiones ZMCM 2004, Gobierno del Distrito Federal, Secretaria del Medio Ambiente, available at: http://www.sma.df.gob.mx/inventario_emisiones/index.php?op=pub#(last access: 29 April 2009), 2004. 11503, 11504
Official Inventory for 2006: Inventario de Emisiones de la ZMVM, 2006, available at: http://www.sma.df.gob.mx/inventario_emisiones/index.php?op=pub#(last access: 29 April 2009), 2008. 11504, 11519
Pougatchev, N. S. and Rinsland, C. P.: Spectroscopic study of the seasonal variation of carbon monoxide vertical distribution above Kitt Peak, J. Geophys. Res., 100, 1409–1416, 1995. 11503, 11509, 11510
Pugacheva, S. G. and Shevchenko, V. V.: The Model of the Moon's Thermal Radiation in the Infrared Spectral Ranges (10–12 Microns), 31st Annual Lunar and Planetary Science Conference, abstract no. 1129, 2000. 11508
Rinsland, C. P. and Levine, J. S.: Free tropospheric carbon monoxide concentrations in 1950 and 1951 deduced from infrared total column amount measurements, Nature, 318, 250–254,

1985. 11503
Rinsland, C. P., Luo, M., Logan, J. A., Beer, R., Worden, H., Kulawik, S. S., Rider, D., Osterman, G., Gunson, M., Eldering, A., Goldman, A., Shephard, M., Clough, S. A., Rodgers, C., Lampel, M., and Chiou, L.: Nadir measurements of carbon monoxide distributions by the Tropospheric Emission Spectrometer instrument onboard the Aura Spacecraft: Overview of analysis approach and examples of initial results, Geophys. Res. Lett., 33L22806, doi:10.1029/2006GL027000, 2006. 11505
Rodgers, C. D.: Retrieval of Atmospheric Temperature and Composition From Remote Measurements of Thermal Radiation, Rev. Geophys., 14(4), 609–624, 1976. 11509
Rodgers, C. D.: Characterization and error analysis of profiles retrieved from remote sounding measurements, J. Geophys. Res., 95, 5587–5595, 1990. 11511
Rodgers, C. D.: Invers methods for atmospheric sounding: Theory und Practice, World Scientific Publishing Co. Pte. Ltd, 2000. 11511
Rothman, L. S., Jacquemart, D., Barbe, A., Benner, C. D., Birk, M., Brown, L. R., Carleer, M. R., Chackerian, C., Chance, K., Coudert, L. H., Dana, V., Devi, V. M., Flaud, J.-M., Gamache, R. R., Goldman, A., Hartmann, J.-M., Jucks, K. W., Maki, A. G., Mandin, J.-Y., Massie, S. T., Orphal, J., Perrin, A., Rinsland, C. P., Smith, M. A. H., Tennyson, J., Tolchenov, R. N., Toth, R. A., Vander Auwera, J., Varanasi, P., and Wagner, G.: The HITRAN 2004 molecular spectroscopic database, J. Quant. Spectrosc. Ra., 96, 139–204, 2005. 11510
Schifter, I., Diaz, L., and Mugica, V., and Lopez-Salinas, E.: Fuel-based motor vehicle emission inventory for the metropolitan area of Mexico city, Atmos. Environ., 39, 931-940, 2005. 11504
Senten, C., De Mazire, M., Dils, B., Hermans, C., Kruglanski, M., Neefs, E., Scolas, F., Vandaele, A. C., Vanhaelewyn, G., Vigouroux, C., Carleer, M., Coheur, P. F., Fally, S., Barret, B., Baray, J. L., Delmas, R., Leveau, J., Metzger, J. M., Mahieu, E., Boone, C., Walker, K. A., Bernath, P. F., and Strong, K.: Technical Note: New ground-based FTIR measurements at Ile de La Runion: observations, error analysis, and comparisons with independent data, Atmos. Chem. Phys., 8, 3483–3508, 2008, http://www.atmos-chem-phys.net/8/3483/2008/. 11503, 11510
Servicio Meteorologico Nacional: Radiosondes daily at 0 and 12 UTC in Mexico City, available at: http://smn.cna.gob.mx(last access: 29 April 2009), 2008. 11510
Shaw, W. J., Pekour, M. S., Coulter, R. L., Martin, T. J., and Walters, J. T.: The daytime mixing layer observed by radiosonde, profiler, and lidar during MILAGRO, Atmos. Chem. Phys. Discuss., 7, 15025–15065, 2007,

http://www.atmos-chem-phys-discuss.net/7/15025/2007/. 11504, 11521
Steck, T.: Methods for determining regularization for atmospheric retrieval problems, Appl. Optics, 41, 1788–1797, 2002. 11509, 11510
Stephens, S., Madronich, S., Wu, F., Olson, J. B., Ramos, R., Retama, A., and Muñoz, R.: Weekly patterns of México City's surface concentrations of CO, NO_x, PM_{10} and O_3 during 1986-2007, Atmos. Chem. Phys., 8, 5313–5325, 2008, http://www.atmos-chem-phys.net/8/5313/2008/. 11503, 11504, 11522
Stremme, W.: Bestimmung hoehenaufgeloester Trends der Spurengase O_3, N_2O und CH_4 mit Hilfe der solaren Infrarotspektroskopie am Standort Zugspitze, Ph.D. thesis, Universität Augsburg, available at: http://www.opus-bayern.de/uni-augsburg/volltexte/2007/551/(last access: 29 April 2009), 2007. 11520
Sussmann, R. and Borsdorff, T.: Technical Note: Interference errors in infrared remote sounding of the atmosphere, Atmos. Chem. Phys., 7, 3537–3557, 2007, http://www.atmos-chem-phys.net/7/3537/2007/. 11511
Sussmann, R. and Buchwitz, M.: Initial validation of ENVISAT/SCIAMACHY columnar CO by FTIR profile retrievals at the Ground-Truthing Station Zugspitze, Atmos. Chem. Phys., 5, 1497–1503, 2005, http://www.atmos-chem-phys.net/5/1497/2005/. 11503, 11510
Sussmann, R., Stremme, W., Burrows, J. P., Richter, A., Seiler, W., and Rettinger, M.: Stratospheric and tropospheric NO_2 variability on the diurnal and annual scale: a combined retrieval from ENVISAT/SCIAMACHY and solar FTIR at the Permanent Ground-Truthing Facility Zugspitze/Garmisch, Atmos. Chem. Phys., 5, 2657–2677, 2005, http://www.atmos-chem-phys.net/5/2657/2005/. 11520
Tikhonov, A.: On the solution of incorrectly stated problems and a method of regularization, Dokl. Akad. Nauk SSSR+, 151, 501–504, 1963. 11509
Turquety, S., Clerbaux, C., Law, K., Coheur, P.-F., Cozic, A., Szopa, S., Hauglustaine, D. A., Hadji-Lazaro, J., Gloudemans, A. M. S., Schrijver, H., Boone, C. D., Bernath, P. F., and Edwards, D. P.: CO emission and export from Asia: an analysis combining complementary satellite measurements (MOPITT, SCIAMACHY and ACE-FTS) with global modeling, Atmos. Chem. Phys., 8, 5187–5204, 2008, http://www.atmos-chem-phys.net/8/5187/2008/. 11503
Velazco, V., Notholt, J., Warneke, T., Lawrence, M., Bremer, H., Drummond, J., Schulz, A., Krieg, J., and Schrems, O.: Latitude and altitude variability of carbon monoxide in the At-

lantic detected from ship-borne Fourier transform spectrometry, model, and satellite data, J. Geophys. Res., 110, D09306, doi:10.1029/2004JD005351, 2005. 11510

von Clarmann, T. and Grabowski, U.: Elimination of hidden a priori information from remotely sensed profile data, Atmos. Chem. Phys., 7, 397–408, 2007, http://www.atmos-chem-phys.net/7/397/2007/. 11509, 11510

von Clarmann, T., Grabowski, U., and Kiefer, M.: On the role of non-random errors in inverse problems in radiative transfer and other applications, J. Quant. Spectrosc. Ra., 71, 39–46, 2001. 11511

Whiteman, C. D., Zhong, S., Bian, X., Fast, J. D., and Doran, J. C.: Boundary layer evolution and regional-scale diurnal circulations over the Mexico Basin and Mexican plateau, J. Geophys. Res., 105, 10 081–10 102, doi:10.1029/2000JD900039, 2000. 11520, 11521

Wiegner, M., Emeis, S., Freudenthaler, V., Heese, B., Junkermann, W., Münkel, C., Schäfer, K., Seefeldner, M., and Vogt, S.: Mixing layer height over Munich, Germany: Variability and comparisons of different methodologies, J. Geophys. Res., 111, 2005JD006593, doi:10.1029/2005JD006593, 2006. 11521

Yurganov, L. N., Blumenstock, T., Grechko, E. I., Hase, F., Hyer, E. J., Kasischke, E. S., Koike, M., Kondo, Y., Kramer, I., Leung, F.-Y., Mahieu, E., Mellqvist, J., Notholt, J., Novelli, P. C., Rinsland, C. P., Scheel, H. E., Schulz, A., Strandberg, A., Sussmann, R., Tanimoto, H., Velazco, V., Zander, R., and Zhao, Y.: A quantitative assessment of the 1998 carbon monoxide emission anomaly in the Northern Hemisphere based on total column and surface concentration measurements, J. Geophys. Res., 109, D15305, doi:10.1029/2004JD004559, 2004. 11503, 11510

Yurganov, L. N., Duchatelet, P., Dzhola, A. V., Edwards, D. P., Hase, F., Kramer, I., Mahieu, E., Mellqvist, J., Notholt, J., Novelli, P. C., Rockmann, A., Scheel, H. E., Schneider, M., Schulz, A., Strandberg, A., Sussmann, R., Tanimoto, H., Velazco, V., Drummond, J. R., and Gille, J. C.: Increased Northern Hemispheric carbon monoxide burden in the troposphere in 2002 and 2003 detected from the ground and from space, Atmos. Chem. Phys., 5, 563–573, 2005, http://www.atmos-chem-phys.net/5/563/2005/. 11503

Yurganov, L. N., McMillan, W. W., Dzhola, A. V., Grechko, E. I., Jones, N. B., and van der Werf, G. R.: Global AIRS and MOPITT CO measurements: Validation, comparison, and links to biomass burning variations and carbon cycle, J. Geophys. Res., 113, D09301, doi:10.1029/2007JD009229, 2008. 11503

Table 1. Smoothing error for two retrievals using different constraints and calculated with different a priori covariances (**Sa**) addressing (a) the urban variability and (b) the regional variability. The Sa is based on a profile ensemble which is constructed from (a) the MLH retrieval results and the surface concentrations and (b) from MOPITT profile retrievals for winter 2007/2008 in the area 102–90° W and 17–21° N, (the relative information is in respect to the average of the retrieved CO column in Mexico City, mean column=3.27×10^{18} molecules/cm^2).

		STDEV	Smoothing error	
			Block VMR	Scaling
(a) 2 Parameter	in (molec/cm^2)	1.07E18	5.9E16	3.2E17
$\epsilon^a_{\text{smooth}}$	% of mean col	32.7	1.81	9.76
(b) MOPITT	in (molec/cm^2)	8.8E16	3.5 E16	2.2 E16
$\epsilon^b_{\text{smooth}}$	% of mean col	2.7	1.08	0.67
Total	in (molec/cm^2)	1.07E18	6.9E16	3.2E17
	% of mean col	32.7	2.1	9.81

ACPD
9, 11501–11549, 2009

Table 2. Overview of the most important errors.

Type of errors Description:	Smoothing $\epsilon^1_{\text{smooth}}\epsilon^2_{\text{smooth}}$	Temperature +5 K all layer	ILS (Sect. 4.3)	Total systematic	Random error measurement	 hourly mean
in (molec/cm^2)	6.9E16	6.5E15	~1E17	1.2E17	1.5E17	3E16
in (%)	2.1	0.2	~2–4	~4	4.9	1.1

ACPD
9, 11501–11549, 2009

Table 3. Results from the retrieved CO column above the mixing layer (Altzomoni site). To avoid the impact of pollution transport detected in the afternoons, only late morning data were used (09:00–12:00 LT).

Column (10^{18} molecules/cm^2)	Overall sun	Daily mean sun (09:00–12:00 LT)	Moon (1 night) (30 Nov/1 Dec)
Minimum	1.04	1.13	1.15
Mean	1.21(±0.09)	1.20(±0.08)	1.26(±0.06)
STDEV	0.087	0.079	0.063

ACPD
9, 11501–11549, 2009

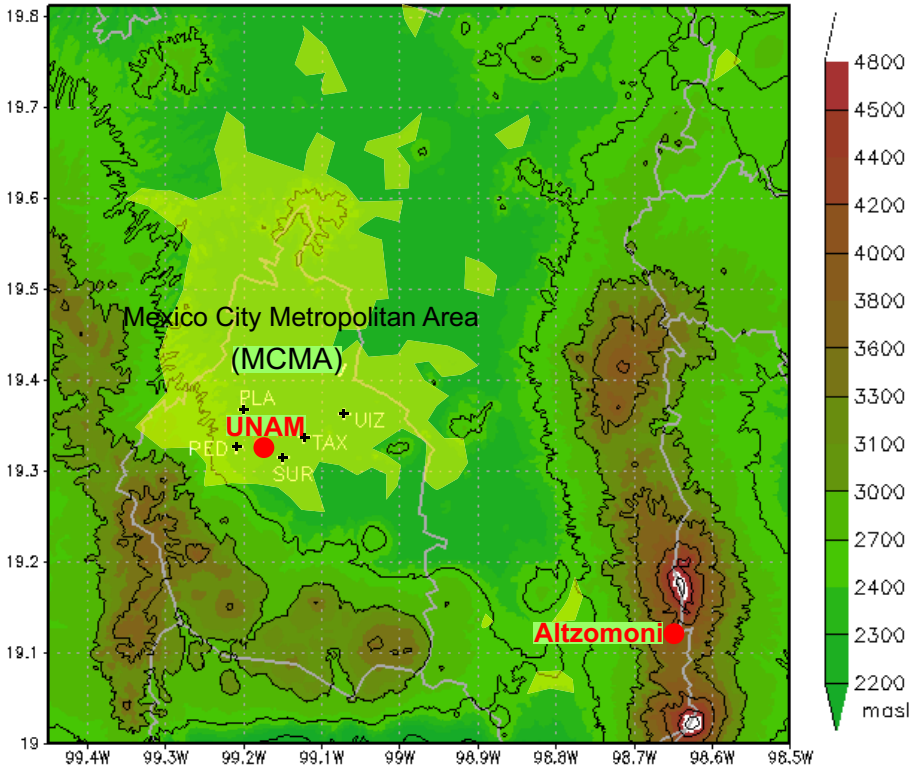

Fig. 1. Topographical map of Mexico City and its surroundings. The yellow area depicts the Mexico City metropolitan area (MCMA) and the red dots indicate the location of the FTIR sites. The black crosses indicate the used monitoring sites (http://www.sma.df.gob.mx/simat/).

ACPD
9, 11501–11549, 2009

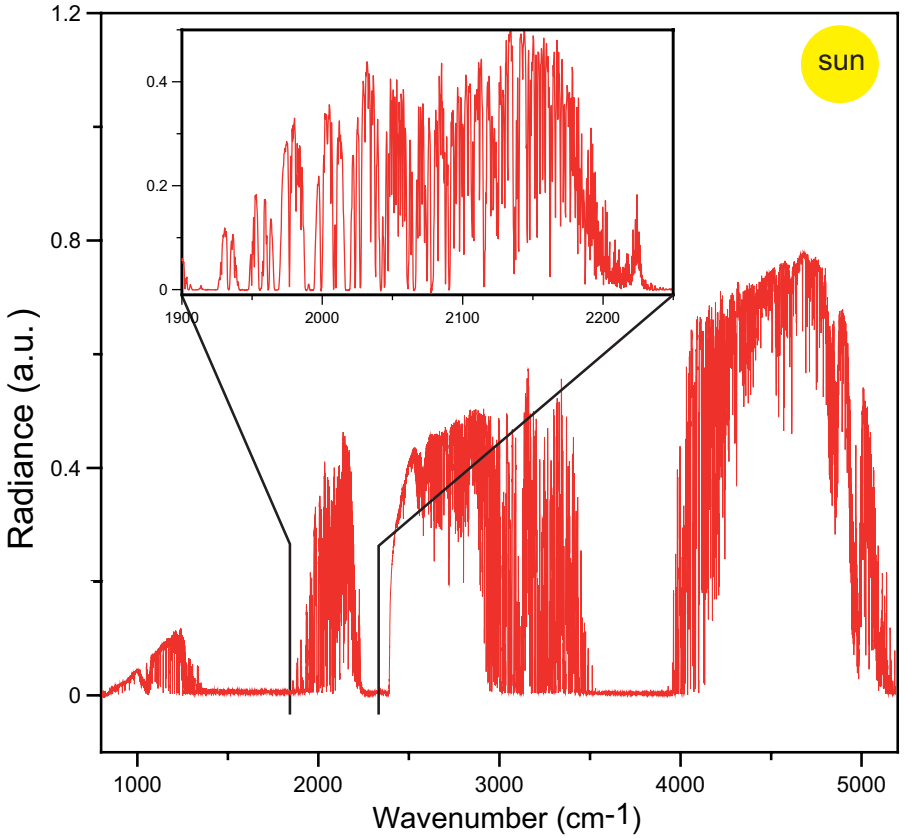

Fig. 2. Typical solar spectrum (large box) recorded at the UNAM site after a background (thermal emission) subtraction (step 2). The small box (inset) shows the same solar spectrum in the region about the CO band after a further CO specific correction (step 3).

ACPD
9, 11501–11549, 2009

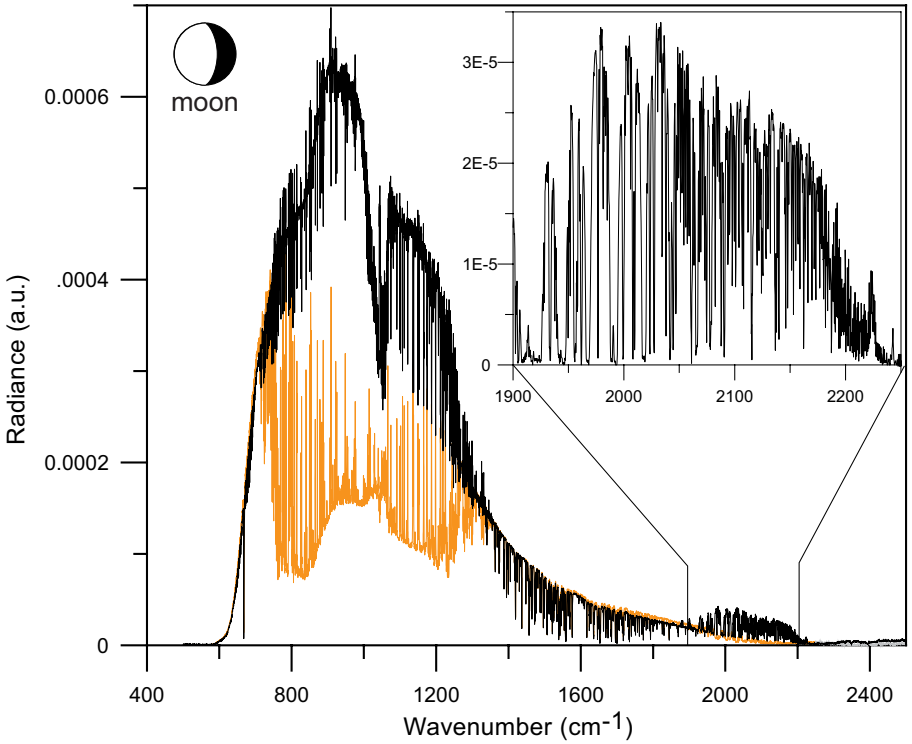

Fig. 3. Lunar spectrum in black (large box) recorded around full moon directly after the Fourier-transformation (step 1) and in orange the atmospheric (+ instrumental) self emission. Moon and thermal emission spectra have to be recorded with the same zenith angle and at almost the same time, so that the atmospheric states are comparable. The corrected lunar spectrum around CO band is shown in the small box (step 3).

ACPD
9, 11501–11549, 2009

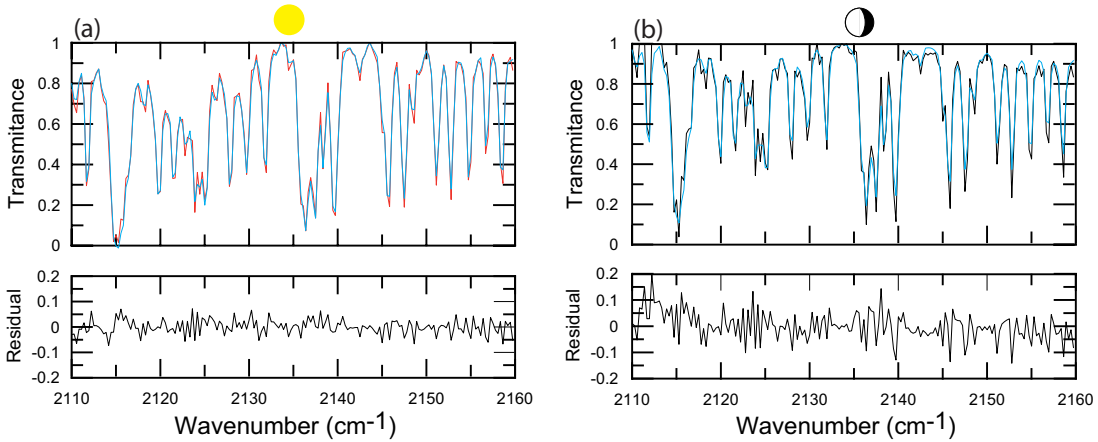

Fig. 4. Example column retrieval of CO from **(a)** solar spectrum taken on 22 January at 10:30 LT. The measured solar spectrum is in red and the simulated spectrum in blue. The retrieved CO column is equivalent to a CO column density of 3.08 molecules/cm^2. **(b)** Example of a lunar CO column (2.74×10^{18} molecules/cm^2) retreived on 24 February at 02:51 LT. The measured lunar spectrum is in black and the simulated spectra in blue. Below are the residuals from the fits.

ACPD
9, 11501–11549, 2009

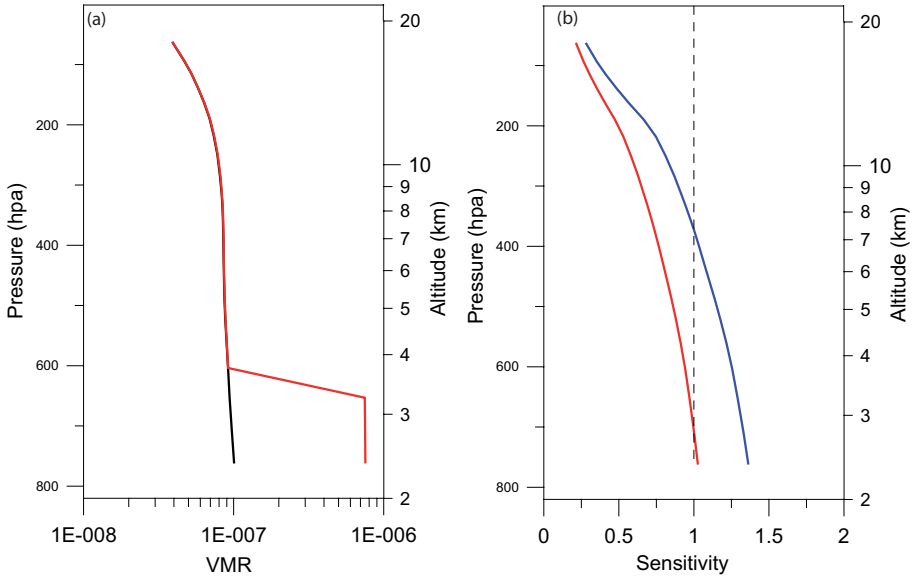

Fig. 5. Left **(a)**: Used a priori profile (black) from MOPITT and retrieved profile (red) on 22 January 2008 at 10:29 LT. Right **(b)**: Total column averaging kernel for the used block constraint (red) and calculated around the retrieved state; the total column kernel but for a scaling constraint is shown in blue.

ACPD
9, 11501–11549, 2009

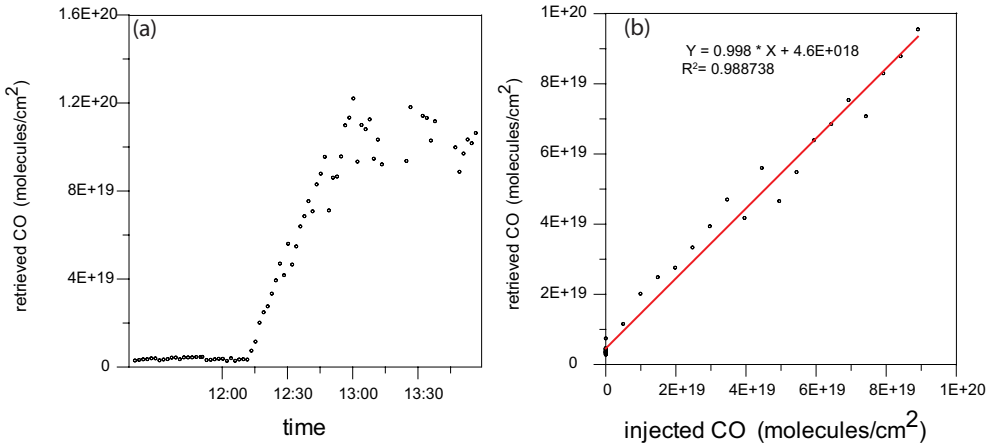

Fig. 6. A controlled experiment designed to prove the linearity of the measured retrieval unit. **(a)** The retrieved CO column is plotted against time after pure CO was being injected into a semi-closed cell (telescope) in constant time intervals during an assumed constant SZA. **(b)**: A correlation plot between the measured and injected CO (250 ml per injection).

ACPD
9, 11501–11549, 2009

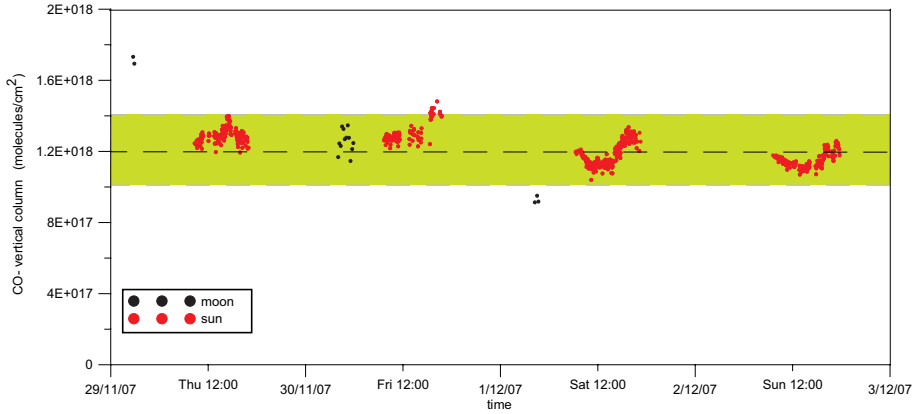

Fig. 7. CO column at the high-altitude site in Altzomoni (19.12° N, 98.65° W, 4010 m a.s.l.) located 60 km southeast of Mexico City. The CO column is retrieved from solar and lunar infrared spectra from 28 November to 2 December 2007. The green bar marks the $1.2\pm0.2\times10^{18}$ molecules/cm^2 area, which is also shown in further figures representing the variability in the regional CO background.

ACPD
9, 11501–11549, 2009

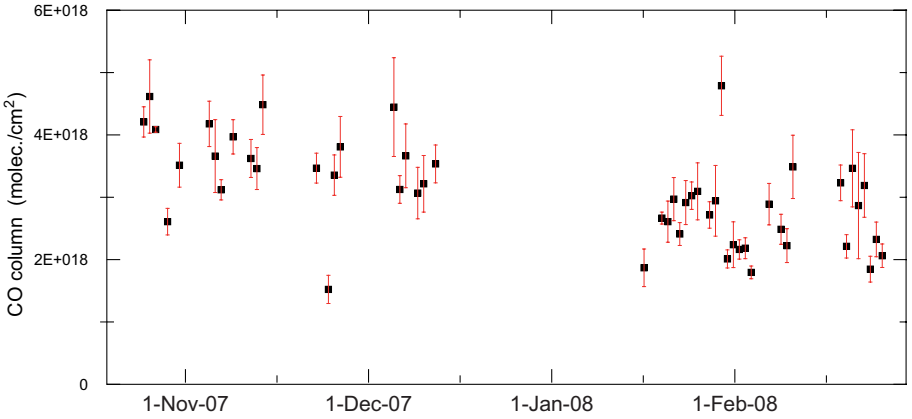

Fig. 8. Time series (15 October 2007 to 27 February 2008) of daily CO column taken from the late morning (9:00-12:00 LT) averages. The red bars show the STDEV of the averaged data.

ACPD
9, 11501–11549, 2009

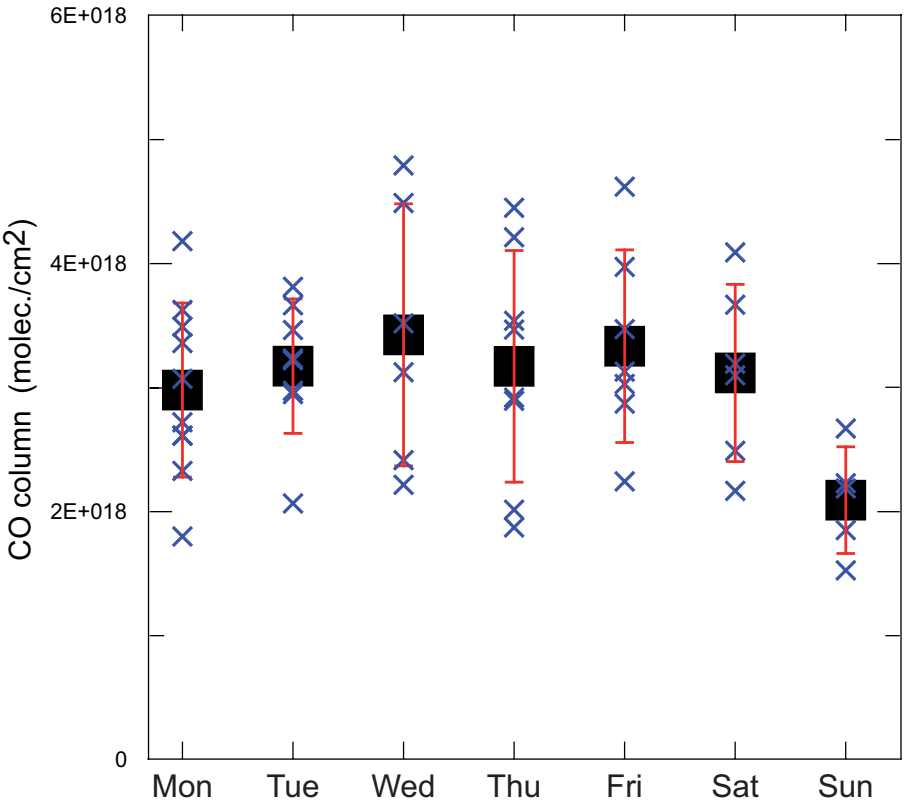

Fig. 9. Blue: Same data (blue) as shown in Fig. 8 but sorted by day of the week. Mean column of a specific weekday (black squares) and the corresponding STDEV (red bars).

ACPD
9, 11501–11549, 2009

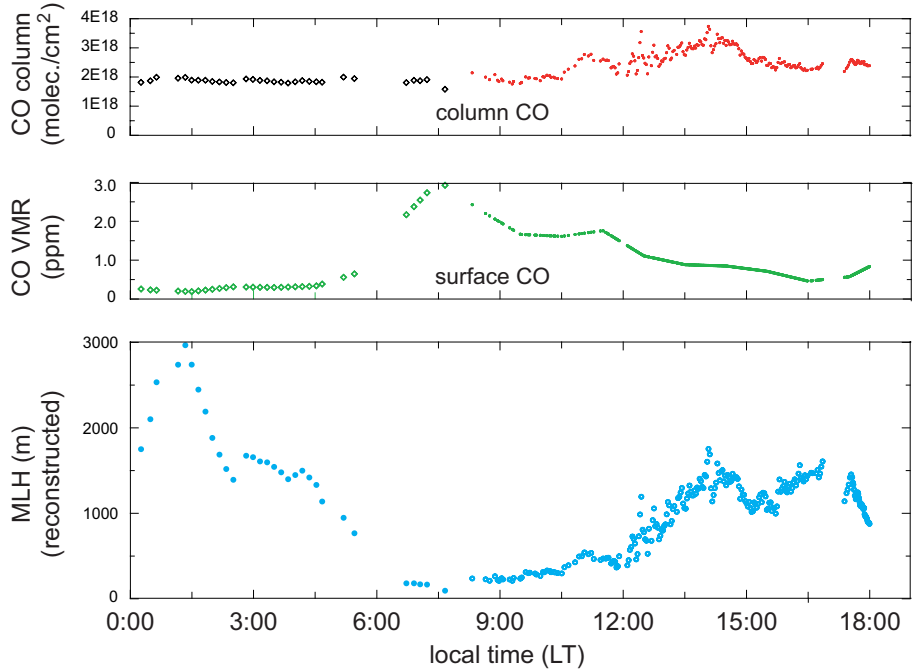

Fig. 10. Example day (25 February 2008) showing the CO column retrieved from lunar (black) and solar (red) IR-spectra (highest graph). CO surface VMR (green, mean of 5 RAMA stations) and the reconstructed effective mixing layer height (blue) are presented in the middle and lower plots.

ACPD
9, 11501–11549, 2009

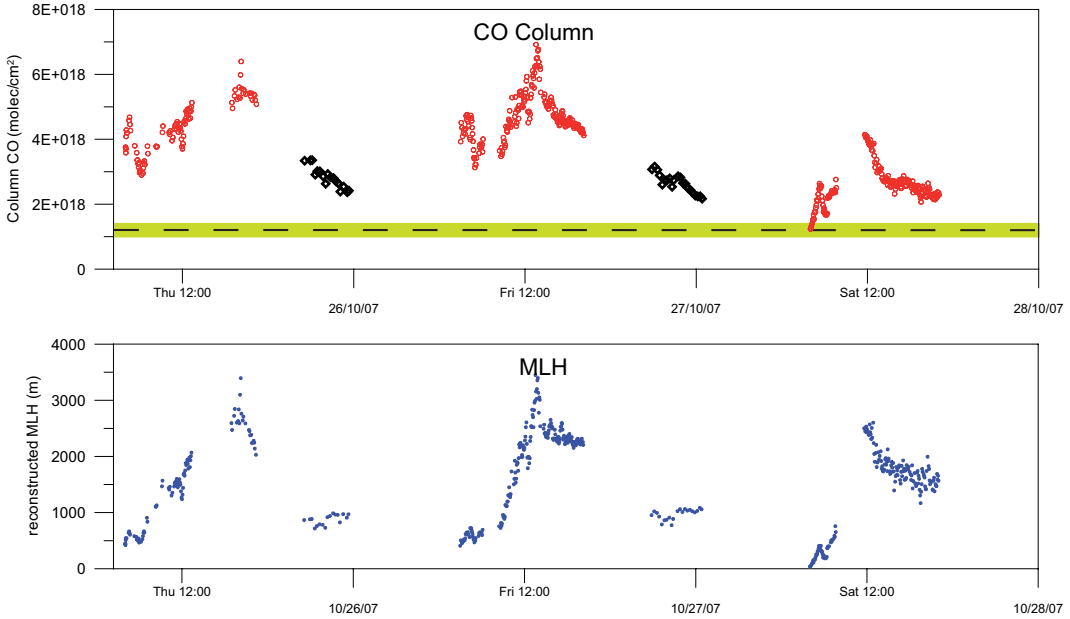

Fig. 11. Retrieved CO column during October 2007 from solar spectra in red and from lunar spectra in black. The estimated effective mixing layer height (blue) is reconstructed from a model which assumes a single layer (green bar, same as Fig. 7)."

ACPD
9, 11501–11549, 2009

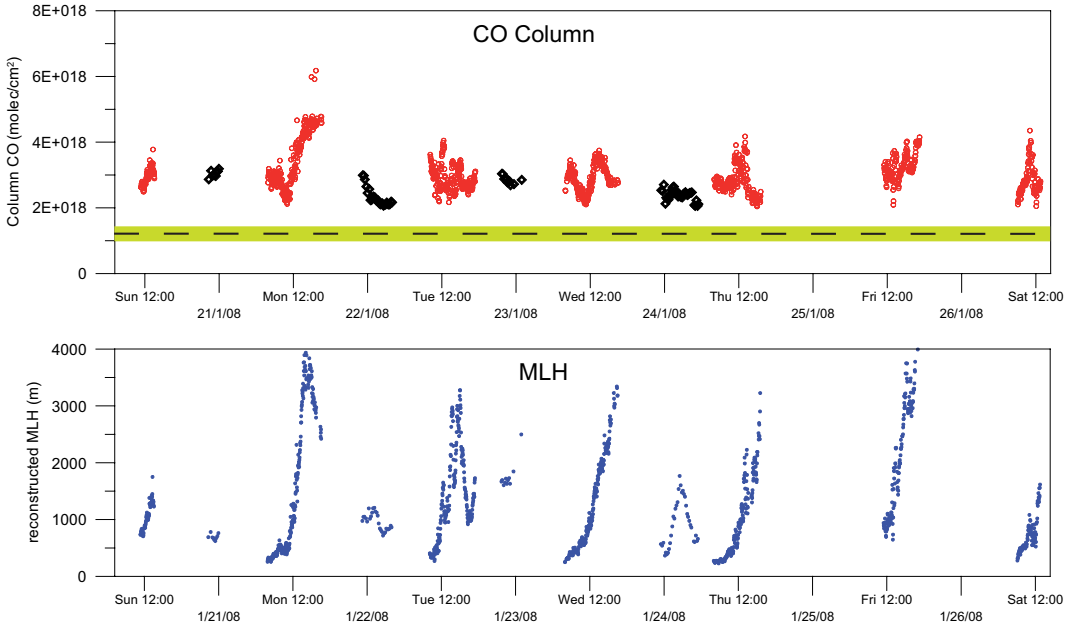

Fig. 12. Same as Fig. 11 but for January 2008 (green bar, same as Fig. 7).

ACPD
9, 11501–11549, 2009

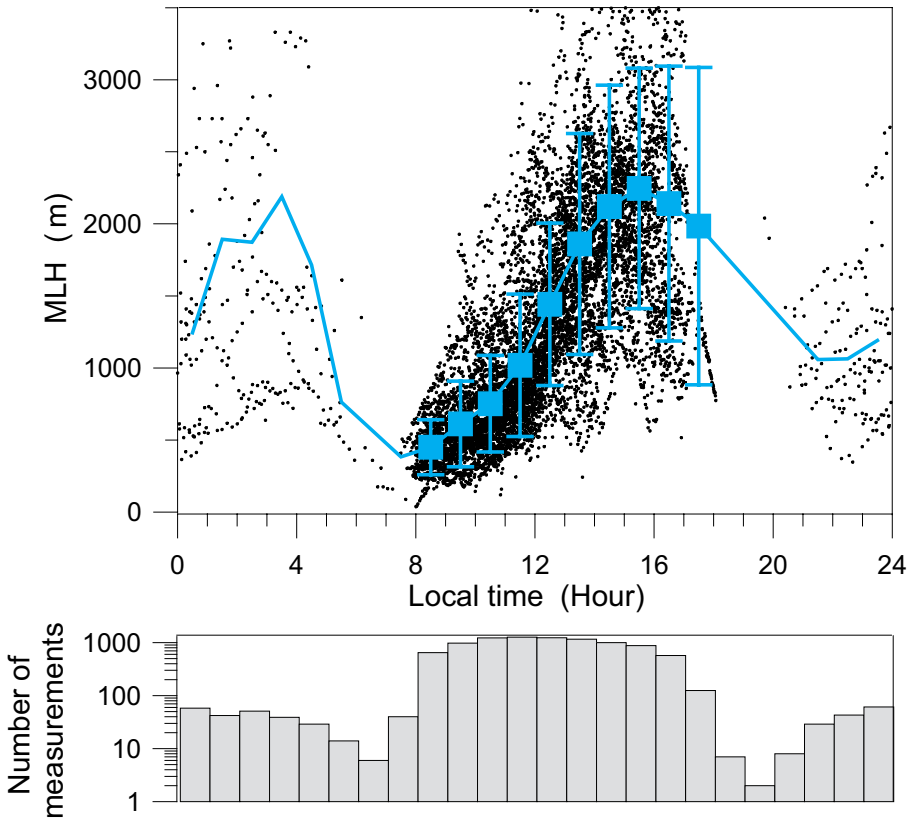

Fig. 13. MLH-averages in the same hour and corresponding STDEV are given in blue squares and bars, respectively (only data with more than 100 measurements). The blue line follows the hourly averages including those times with 10 measurements or more, as gathered from the statistical chart in the bottom.

ACPD
9, 11501–11549, 2009

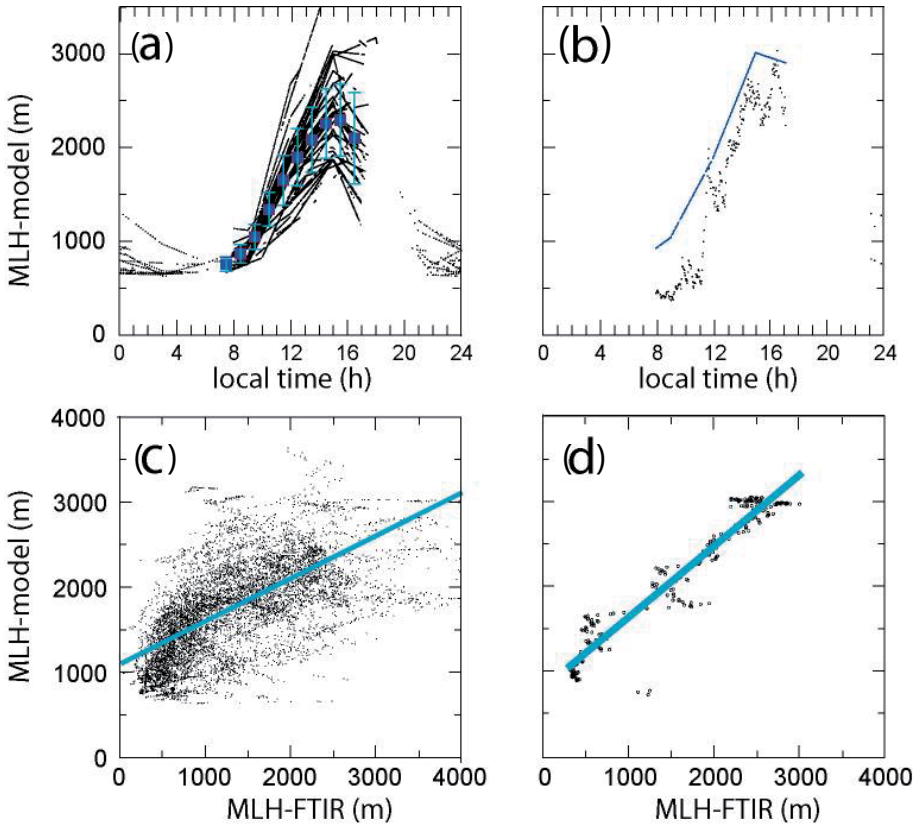

Fig. 14. Dirunal change in mixing layer height. **(a)** Same as Fig. 13 but for model data (NCEP, 2008[2]) interpolated to the measurement times; **(b)** MLH traces for a single day where the FTIR-retreived MLH is black and from the model is blue. Below: Correlation between model and FTIR-retreived MLH. **(c)** all data, **(d)** for the same single day as shown in plot **(b)**.

ACPD
9, 11501–11549, 2009